ELSEVIER

Manganese(II) complexes of a set of 2-aminomethylpyridine-derived ligands bearing a methoxyalkyl arm: syntheses, structures and magnetism

Jian-Zhong Wu [a,1], Elisabeth Bouwman [a,*], Allison M. Mills [b], Anthony L. Spek [b], Jan Reedijk [a]

[a] *Leiden Institute of Chemistry, Gorlaeus Laboratories, Leiden University, P.O. Box 9502, 2300 RA Leiden, The Netherlands*
[b] *Bijvoet Center for Biomolecular Research, Department of Crystal and Structural Chemistry, Utrecht University, Padualaan 8, 3584 CH Utrecht, The Netherlands*

Abstract

Four new ligands, *N*-(2-methoxyethyl)-*N*-(pyridin-2-ylmethyl)amine (mepma), *N*-(3-methoxypropyl)-*N*,*N*-bis(pyridin-2-ylmethyl)-amine (mpbpa), *N*-(2-methoxyethyl)-*N*,*N*-bis(pyridin-2-ylmethyl)amine (mebpa) and 2-{[(2-methoxyethyl)(pyridin-2-ylmethyl)amino]methyl} phenol (Hmepap), and four of their complexes with manganese(II) halides, [MnCl$_2$(mepma)$_2$] (**1**), [MnCl(μ-Cl)(mpbpa)]$_2$ (**2**), [MnBr$_2$(mebpa)] (**3**) and [MnBr$_2$(MeOH)(Hmepap)] (**4**) have been synthesized and characterized. Single-crystal Xray studies revealed that in all four complexes, the Mn(II) coordination spheres are distorted octahedral. In **1** and **2**, the ether oxygen atom does not coordinate to the Mn(II) centre, but in **3** and **4** it does. The mononuclear molecules of **1** are linked by double hydrogen bonds to form linear chains. Temperature dependent magnetic susceptibility measurements revealed that the Mn(II) ions in **1** interact anti-ferromagnetically, with $J = -1.06$ cm^{-1}. Compound **2** crystallizes as a double chloride-bridged dimer in which there is a weak ferromagnetic interaction ($J = 0.55$ cm^{-1}) between the Mn(II) pair. The solution EPR spectrum of **2** suggests that in methanol compound **2** decomposes to a great extent to mononuclear species. In compound **3**, mebpa acts as a tetradentate ligand with all of its nitrogen and oxygen atoms coordinated to the Mn(II) ion. Unexpectedly, in complex **4**, the phenolic oxygen of Hmepap remains protonated and does not coordinate to the metal ion. Instead the oxygen from a methanol molecule coordinates the manganese centre. Hydrogen bonds between one of the two bromide ions, and the methanol and phenol hydroxyl groups, respectively, connect the mononuclear molecules of **4** into chains. No magnetic interactions were observed between the Mn(II) ions in **3** or **4**.
© 2004 Elsevier B.V. All rights reserved.

Keywords: Manganese; Pyridine; Phenol; Ether; Magnetism

1. Introduction

The coordination chemistry of manganese with N and/or O containing ligands has recently been receiving a great deal of attention, because of the variable structures of manganese complexes, the wide occurrence of manganese enzymes in plants and bacteria [1–4], the possibility of magnetic coupling interactions [5–7], and the application of manganese compounds in industrial catalysis, for example epoxidation [8–10], bleaching [11] and paint drying [12,13]. The behaviour of these manganese complexes is mainly dependent on the structure and coordination mode of the ligands in addition to the oxidation number of manganese. Various manganese complexes with 2-aminomethylpyridine or its derivatives have been studied with respect to their structures and properties [14–19]. Herein, we report the synthesis and magnetic properties of some new ligands derived from 2-aminomethylpyridine (Scheme 1) and some of their manganese(II) complexes. The ligand mebpa and its Fe(III) complex has been reported earlier [20].

* Corresponding author. Tel.: +31-71-5274550; fax: +31-71-5274451.
E-mail address: bouwman@chem.leidenuniv.nl (E. Bouwman).
[1] Present address: Department of Chemistry, South China Normal University, China.
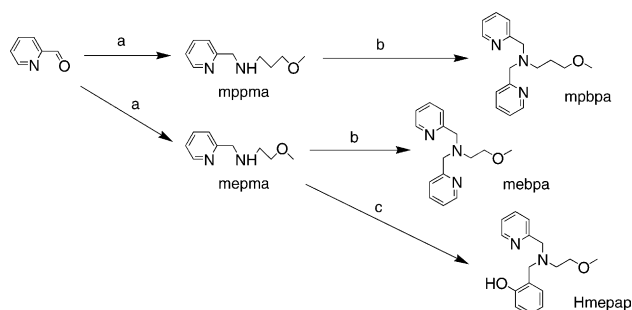
Scheme 1. Synthesis of the ligands: (a) methoxyalkylamine, toluene; NaBH₄, (b) picolyl chloride, K₂CO₃, acetonitrile, (c) salicyl aldehyde, methanol; NaBH₄.

2. Experimental

2.1. General methods

All reagents were purchased from commercial sources and used as received. All solvents were purified by regular methods. The syntheses were performed under an inert atmosphere of argon using standard Schlenk equipment. X-band EPR spectra were recorded on a Jeol RE2x electron spin resonance spectrometer using DPPH ($g = 2.0036$) as a standard. FTIR spectra were obtained on a Perkin–Elmer Paragon 1000 FTIR spectrophotometer equipped with a Golden Gate ATR device, using the diffuse reflectance technique (4000–300 cm^{-1}, resolution, 4 cm^{-1}). C, H, and N determinations were performed on a Perkin Elmer 2400 Series II analyzer. NMR spectra were recorded on a JEOL JNM FX-200 (200 MHz) instrument. Mass spectrometry experiments were performed on a Finnigan MAT TSQ-700 equipped with a custom-made electrospray interface (ESI). Magnetic susceptibility measurements (2–300 K) were carried out (at 1000 G) using a Quantum design MPMS-5 5T SQUID magnetometer. Data were corrected for the magnetization of the sample holder and for diamagnetic contributions, which were estimated from the Pascal constants [5].

2.2. Synthesis

The synthesis of mppma, N-(3-methoxypropyl)-N-(pyridin-2-ylmethyl)amine, has recently been described [19].

2.2.1. N-(2-methoxyethyl)-N-(pyridin-2-ylmethyl)amine (mepma)

A solution of 2-pyridinecarboxaldehyde (5.24 g, 48.9 mmol) and one equivalent of 3-methoxypropylamine (3.70 g) in 110 ml of toluene was refluxed under argon overnight, in a flask equipped with a Dean-Stark separator. The solvent was removed using a rotating evaporator, and to the residue oil was added 80 ml of

methanol, followed by 1.87 g (48.9 mmol) sodium borohydride in portions with stirring. Subsequently, the solution was continuously stirred for 5 h. Hydrochloric acid (10%) was added to destroy unreacted sodium borohydride until a pH of ca. 7 was reached. Then sodium hydroxide solution (10%) was added to adjust the pH to about 10. The solvent was removed and 10 ml of water was added to the residue. The solution was extracted with 4 × 20 ml of diethyl ether. The extract was dried with anhydrous sodium sulfate. After removing the diethyl ether, the product was isolated as orange oil. Yield: 7.86 g (96%). ^{1}H NMR (CDCl₃): δ (ppm) 8.44 (d, 1H, pyC6H), 7.53 (t, 1H, pyC4H), 7.22 (d, 1H, pyC3H), 7.05 (t, 1H, pyC5H), 3.83 (s, 2H, py–CH₂–N), 3.43 (t, 2H, CH₂–CH₂–O), 3.26 (s, 3H, O–CH₃), 2.74 (t, 2H, N–CH₂–CH₂), 2.53 (br, NH). ^{13}C NMR (CDCl₃): δ (ppm) 159.5 (pyC2), 149.0 (pyC6), 136.2 (pyC4), 122.0 (pyC3), 121.6 (pyC5), 71.8 (CH₂–CH₂–O), 58.5 (py–CH₂–N), 54.9 (O–CH₃), 48.6 (N–CH₂–CH₂). IR: ν (cm^{-1}) 3320 (br, w), 2880 (m), 2824 (m), 1591 (s), 1570 (m), 1474(m), 1457 (m), 1434 (s), 1111 (s), 1048 (w), 994 (w), 845 (w), 757 (s), 631 (m), 526 (s). MS: 167.0 [M + H]$^+$, 80%.

2.2.2. N-(3-methoxypropyl)-N,N-bis(pyridin-2-ylmethyl)-amine (mpbpa)

A mixture of mppma (454 mg, 2.52 mmol), 2-picolyl chloride hydrochloride (416 mg, 2.53 mmol) and potassium carbonate (704 mg, 5.10 mmol) in 4 ml of acetonitrile was refluxed overnight and the solvent was removed using a rotating evaporator. The residue was taken up into 15 ml of water and 10 ml of dichloromethane and the mixture was made alkaline to pH ca. 9 with ammonia. After separation of the layers, the aqueous layer was extracted with 5 × 30 ml of dichloromethane. The combined organic layers were dried with anhydrous sodium sulfate. After removing the solvent, mpbpa was obtained as orange red oil. Yield: 602 mg (88%). ^{1}H NMR (CDCl₃): δ (ppm) 8.49 (d, 2H, pyC6H), 7.62 (t, 2H, pyC4H), 7.49 (d, 2H, pyC3H), 7.11 (t, 2H, pyC5H), 3.79 (s, 4H, py–CH₂–N), 3.35 (t, 2H, CH₂–CH₂–O), 3.23 (s, 3H, O–CH₃), 2.61 (t, 2H, N–CH₂–CH₂), 1.80 (m, 2H, N–CH₂–CH₂). ^{13}C NMR (CDCl₃): δ (ppm) 159.3 (pyC2), 148.4 (pyC6), 135.8 (pyC4), 122.2 (pyC3), 121.3 (pyC5), 70.3 (CH₂–CH₂–O), 59.9 (O–CH₃), 57.9 (py–CH₂–N), 50.8 (N–CH₂–CH₂), 26.8 (N–CH₂–CH₂). IR: ν (cm^{-1}) 3416 (br, w), 2926 (w), 1661 (w), 1591 (w), 1570 (w), 1475 (w), 1435 (w), 1366 (w), 1117 (m), 890 (w), 760 (w), 631 (m), 530 (s), 490 (s), 389(s). MS: 272.2 [M + H]$^+$, 100%.

2.2.3. N-(2-methoxyethyl)-N,N-bis(pyridin-2-ylmethyl) amine (mebpa)

A mixture of mepma (916 mg, 5.52 mmol), 2-picolyl chloride hydrochloride (903 mg, 5.51 mmol) and potassium carbonate (1.53 g, 11.1 mmol) in 5 ml of acetonitrile was refluxed for 9 h. After cooling, the

mixture was filtered. Acetonitrile was removed from the filtrate and the residue was taken up into 30 ml of water and 20 ml of chloroform, and the mixture was made alkaline to pH ca. 8 with a 10% solution of sodium hydroxide. After separation of the layers, the aqueous layer was extracted with 6×30 ml of chloroform. The combined organic layers were dried with anhydrous sodium sulfate. After removing the solvent, mebpa was obtained as orange red oil. Yield: 1.11 g (78%). ^{1}H NMR (CDCl$_3$): δ (ppm) 8.52 (d, 4H, pyC6H), 7.65 (t, 4H, pyC4H), 7.57 (d, 4H, pyC3H), 7.14 (t, 4H, pyC5H), 3.94 (s, 4H, py–CH_2–N), 3.55 (t, 2H, CH_2–CH$_2$–O), 3.29 (s, 3H, O–CH_3), 2.85 (t, 2H, N–CH_2–CH$_2$). ^{13}C NMR (CDCl$_3$): δ (ppm) 159.3 (pyC2), 148.9 (pyC6), 136.3 (pyC4), 123.0 (pyC3), 121.9 (pyC5), 70.8 (CH$_2$–CH$_2$–O), 60.7 (py–CH$_2$–N), 58.7 (O–CH$_3$), 53.6 (N–CH$_2$–CH$_2$). IR: ν (cm^{-1}) 2820 (m), 1590 (s), 1570 (m), 1473 (m), 1435 (s), 1364 (w), 1198 (w), 1113 (s), 1048 (w), 996 (w), 760 (s), 631 (m), 532 (vs). MS: 258.2 [M + H]$^+$, 100%.

2.2.4. 2-{[(2-methoxyethyl)(pyridin-2-ylmethyl)amino]-methyl}phenol (Hmepap)

A solution of mepma (989 mg, 5.96 mmol) and equivalent salicylaldehyde (730 mg) in 5 ml of methanol was stirred at room temperature for 15 h. Sodium borohydride (225 mg, 5.96 mmol) was added in small portions. After addition, the mixture was stirred for 3 h. Hydrochloric acid (10%) was used to destroy unreacted sodium borohydride to pH ca. 7. Then sodium hydroxide solution (10%) was added to adjust the pH to 8–9. The solvent was removed and 15 ml of water was added. The solution was extracted with 4×20 ml of dichloromethane. The extract was dried with anhydrous sodium sulfate. After filtration and volume reduction, the dichloromethane solution was loaded on a silica gel. Elution by ethyl acetate gave pure product as light yellow oil (subsequent elution by methanol gave unreacted mepma). Yield: 680 mg (42%). ^{1}H NMR (CDCl$_3$): δ (ppm) 7.95 (d, 1H, pyC6H), 7.07 (t, 1H, pyC4H), 6.75 (d, 1H, pyC3H), 6.57 (m, 2H, pyC5H+ phenolC5H), 6.42 (d, 1H, phenolC3H), 6.27 (d, 1H, phenolC6H), 6.18 (t, 1H, phenolC4H), 3.29 (s, 2H, py–CH_2–N), 3.25 (s, 2H, phenol–CH_2–N), 2.93(t, 2H, CH_2–CH$_2$–O), 2.70 (s, 3H, O–CH_3), 2.20 (t, 2H, N–CH_2–CH$_2$). ^{13}C NMR (CDCl$_3$): δ (ppm) 157.8 (pyC2), 157.6 (phenol-C1), 148.9 (pyC6), 136.6 (pyC4), 129.2 (phenol-C3), 128.8 (phenol-C5), 123.5 (phenol-C2), 122.4 (pyC2), 122.3 (phenol-C4), 119.0 (pyC5), 116.3 (phenol-C6), 70.1 (CH$_2$–CH$_2$–O), 60.0 (py–CH$_2$–N), 58.7 (N–CH$_2$–CH$_2$), 57.6 (O–CH$_3$), 52.7 (phenol–CH$_2$–N). IR: ν (cm^{-1}) 2824 (m), 1589 (s), 1571 (w), 1488(s), 1436 (m), 1365 (m), 1250 (s), 1150 (w), 1109 (s), 1037 (w), 846 (w), 754 (s), 632 (m), 532 (s). MS: 273.2 [M + H]$^+$, 100%.

2.2.5. [MnCl$_2$(mepma)$_2$] (1)

A solution of MnCl$_2 \cdot$2H$_2$O (45.7 mg, 0.285 mmol) and mepma (107.4 mg, 0.647 mmol) in 2 ml of methanol was heated at 50 °C for 3 h. After cooling, diethyl ether was added until saturation. After 1 day, pale yellow crystals were collected. Yield: 67.3 mg (52%). *Anal*. Calc. for C$_{18}$H$_{28}$Cl$_2$MnN$_4$O$_2$: C, 47.18; H, 6.16; N, 12.23. Found: C, 46.39; H, 6.99; N, 12.36%. IR: ν (cm^{-1}) 3218 (m), 3062 (w), 2986 (m), 2954 (w), 2926 (w), 2838 (m), 1603 (s), 1570 (m), 1484 (m), 1437 (s), 1393 (w), 1356 (w), 1312 (w), 1285 (m), 1225 (w), 1194 (m), 1150 (m), 1121 (s), 1098 (s), 1054 (m), 1023 (s), 1014v (s), 966 (m), 916 (m), 892 (s), 821 (s), 778 (vs), 737 (s), 668 (m), 644 (m), 624 (m), 551 (w), 490 (m), 416 (s) 396 (w), 310 (w).

2.2.6. [MnCl(μ-Cl)(mpbpa)]$_2$ (2)

A solution of MnCl$_2 \cdot$2H$_2$O (36.2 mg, 0.224 mmol) and mpbpa (63.6 mg, 0.234 mmol) in 4 ml of methanol was heated at 60 °C for 3 h. After cooling, diethyl ether was added until saturation. After 2 days, colourless crystals were collected. Yield: 52.7 mg (52%). *Anal*. Calc. for C$_{32}$H$_{42}$Cl$_4$Mn$_2$N$_6$O$_2$: C, 48.38; H, 5.33; N, 10.58. Found: C, 49.50; H, 5.76; N, 10.65%. IR: ν (cm^{-1}) 3348 (br,m), 2934 (w), 1626 (w), 1603 (s), 1570 (m), 1478 (m), 1440 (s), 1429 (s), 1382 (w), 1311 (w), 1301 (w), 1222 (w), 1198 (w), 1158 (m), 1100 (s), 1048 (s), 1014 (s), 985 (w), 956 (w), 917 (w), 896 (w), 886 (w), 862 (w), 842 (w), 779 (s), 768 (s), 729 (w), 674 (w), 638 (m), 570 (w), 472 (br,s), 412 (s), 322 (m), 302 (m).

2.2.7. [MnBr$_2$(mebpa)] (3)

A solution of MnBr$_2 \cdot$4H$_2$O (28.4 mg, 0.099 mmol) and mebpa (52.8 mg, 0.201 mmol) in 2 ml of methanol was heated at 60 °C for 2 h. After cooling, diethyl ether was added until saturation. After 8 days, colourless crystals were collected. Yield: 35.4 mg (76%). *Anal*. Calc. for C$_{15}$H$_{19}$Br$_2$MnN$_3$O: C, 38.16; H, 4.06; N, 8.90. Found: C, 38.73; H, 4.67; N, 8.93%. IR: ν (cm^{-1}) 3054 (w), 2904 (w), 1601 (s), 1570 (m), 1472 (m), 1438 (s), 1387 (w), 1346 (w), 1304 (m), 1292 (m), 1202 (w), 1155 (w), 1123 (m), 1088 (s), 1046 (s), 1015 (vs), 982 (w), 958 (w), 908 (w), 854 (m), 838 (m), 806 (m), 771 (vs), 731 (m), 638 (s), 568 (w), 512 (w), 489 (m), 417 (s), 340 (w), 310 (w).

2.2.8. [MnBr$_2$(MeOH)(Hmepap)] (4)

A solution of MnBr$_2 \cdot$4H$_2$O (26.4 mg, 0.092 mmol) and Hmepap (26.0 mg, 0.0956 mmol) in 3 ml of methanol was heated at 50 °C for 15 h. After cooling, diethyl ether was added until saturation. After 4 days, colourless crystals were collected. Yield: 32.3 mg (68%). *Anal*. Calc. for C$_{17}$H$_{24}$Br$_2$MnN$_2$O$_3$: C, 39.33; H, 4.66; N, 5.40. Found: C, 38.55; H, 5.43; N, 5.54%. IR: ν (cm^{-1}) 3278 (br,m), 2938 (w), 1606 (m),1593 (m), 1560 (w), 1484 (w),

1456 (s), 1445 (s), 1351 (m), 1338 (m), 1308 (m), 1278 (m), 1252 (w), 1227 (m), 1177 (w), 1158 (m), 1112 (m), 1094 (s), 1070 (s), 1039 (s), 1014 (s), 1004 (vs), 965 (s), 933 (m), 870 (s), 842 (s), 794 (m), 772 (s), 760 (vs), 722 (m), 639 (s), 613 (s), 584 (s), 495 (m), 416 (m), 356 (m), 313 (m).

2.3. Crystallography and structure solution

Intensity data for single crystals of **1**–**4** were collected using graphite-monochromated Mo Kα radiation, on a Nonius KappaCCD diffractometer. A multi-scan absorption correction was applied using PLATON/MULABS (0.765–0.855 transmission for **1**; 0.851–0.909 transmission for **2**; 0.310–0.374 transmission for **3**; 0.231–0.331 transmission for **4**) [21]. The structures were solved by automated Patterson methods using DIRDIF 99 [22], and refined on F^2 using SHELXL 97 [23].

The methoxyethyl chain of the mebpa ligand in **3** is disordered over two conformations. All non-hydrogen atoms were refined with anisotropic displacement parameters. The hydroxyl hydrogen atoms in **4** were positively identified in a difference Fourier map, and were freely refined with an isotropic displacement parameter. All other hydrogen atoms were constrained to idealized geometries and allowed to ride on their carrier atoms with an isotropic displacement parameter related to the equivalent displacement parameter of their carrier atoms. Structure validation and molecular graphics preparation were performed with the PLATON package [21]. Crystallographic data of the structures **1**–**4** are summarized in Table 1.

3. Results and discussion

3.1. Synthesis and IR spectra

The mepma ligand was synthesized in a similar way to mppma [19]. The synthetic methods for the preparation of mebpa, mpbpa and Hmepap included reductive amination reactions as described for related ligands [24]. Under an inert atmosphere, these ligands readily formed light coloured manganese(II) complexes. For complex **3**, although a 1:2 ratio of Mn(II) to mebpa was applied, the elemental analyses and X-ray structure revealed that mebpa coordinates to Mn(II) in 1:1 ratio. The formulae of the other complexes were consistent with the manganese/ligand molar ratios used during synthesis. The four complexes seem to be air-stable in the solid state. However, solutions of the complexes become dark when exposed to air, indicating rapid oxidation of the manganese(II) ion.

All of the ligands and complexes exhibit a characteristic ether vibration band near 1100 cm^{-1} in their IR spectra. Although a shift in the energy of this band upon coordination of the ligand could theoretically be used to judge whether the ether oxygen atom is coordinated to the manganese ion it does not seem to be an absolute criterion [19,25]. For example, after complexation the ether band of mebpa undergoes a red shift from 1113 to 1088 cm^{-1} in crystalline [MnBr$_2$(mebpa)] (**3**), consistent with the observed coordination of the ether oxygen of mebpa to Mn(II) (vide infra). A similar red shift occurs in the case of mepma, i.e., from 1111 cm^{-1} in the free ligand to 1098 cm^{-1} in [MnCl$_2$(mepma)$_2$] (**1**), however, in this case the crystal structure clearly shows that the ether oxygen is not coordinated (vide infra).

Table 1
Crystallographic data for the structures of **1**–**4**

	1	**2**	**3**	**4**
Formula	$C_{18}H_{28}Cl_2MnN_4O_2$	$C_{32}H_{42}Cl_4Mn_2N_6O_2$	$C_{15}H_{19}Br_2MnN_3O$	$C_{17}H_{24}Br_2MnN_2O_3$
Formula weight	458.28	794.40	472.09	519.14
Crystal system	orthorhombic	monoclinic	monoclinic	triclinic
Space group	$Pccn$ (No. 56)	$P2_1/c$ (No. 14)	$P2_1/c$ (No. 14)	P (No. 2)
a (Å)	17.2693(3)	9.5514(4)	8.2765(1)	9.4560(2)
b (Å)	9.7537(1)	15.2800(6)	26.1586(4)	10.0621(2)
c (Å)	12.9363(2)	13.6667(7)	9.0655(1)	11.2142(2)
α (°)	90	90	90	106.1111(7)
β (°)	90	118.604(3)	116.9146(6)	96.7446(6)
γ (°)	90	90	90	93.4605(7)
V (Å^3)	2178.98(6)	1751.15(13)	1750.10(4)	1013.16(3)
Z	4	2	4	2
D_{calc} (g cm^{-3})	1.397	1.507	1.792	1.702
$F(000)$	956	820	932	518
μ(Mo Kα) (cm^{-1})	8.71	10.65	53.24	46.13
T (K)	150	150	150	150
R_1	0.0248	0.0343	0.0413	0.0327
wR_2	0.0647	0.0747	0.1169	0.0866
S	1.050	1.023	1.047	1.040

3.2. Description of the structures

3.2.1. [MnCl₂(mepma)₂] (1)

The molecular structure of **1** is shown in Fig. 1. Se-
lected bond lengths and angles are listed in Table 2. The
six-coordinate manganese(II) ion centres a C_2-symmet-
ric distorted octahedron; the two chloride anions occupy
cis positions, while the two amine and two pyridine ni-
trogen atoms are *cis* and *trans* with respect to each
other, repectively. The oxygen atom of the methoxyethyl
arm of mepma does not coordinate to the Mn(II) ion,
despite the potential of forming a five-membered chelate
ring. The [MnCl₂(mepma)₂] monomers are linked by
two equivalent N–H···Cl hydrogen bonds per molecule
[N(18)···Cl(1a) (a: $x, 1/2 - y, 1/2 + z) = 3.4974(11)$ Å]
to form 1D chains that run along the *c*-direction, as
shown in Fig. 2.

The analogous ligand mppma, with a methoxypropyl
arm instead of the methoxyethyl arm of mepma, forms a
polymeric chain formulated as [Mn(μ-Cl)₂(mppma)]ₙ
when combined with MnCl₂ [19]. In this compound, as
in **1**, the ether oxygen of the mppma ligand remains
uncoordinated.

The Mn(1)–N(11) and Mn(1)–N(18) distances in **1** are
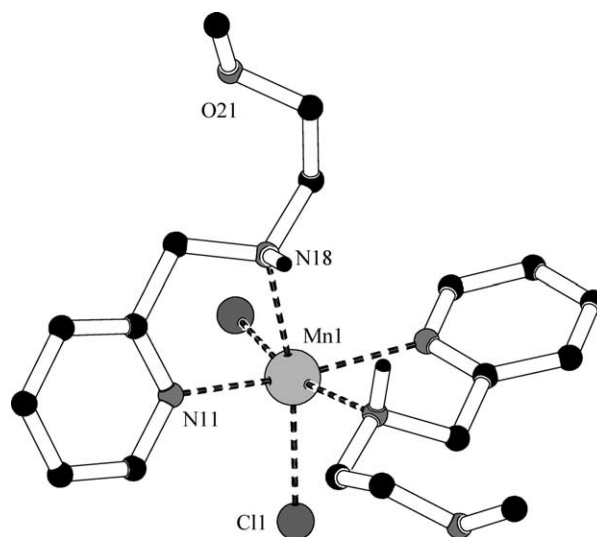2.2885(11) and 2.3557(11) Å, respectively, reflecting the

Fig. 1. PLATON projection of **1** with relevant labelling. Hydrogen
atoms, except the one attached to the amine nitrogen, have been
omitted for clarity.

stronger coordinating ability of the pyridine nitrogen
versus that of the nitrogen of the aliphatic secondary
amine, as observed for [Mn(μ-Cl)₂(mppma)]ₙ
[2.2426(16) and 2.3381(16) Å, respectively] [19]. The

Table 2
Selected bond lengths (Å) and angles (°) in the structures **1**–**4**

| For **1** (a: $1/2 - x, 1/2 - y, z$)					
Mn1–Cl1	2.4810(4)	Mn1–N11	2.2885(11)	Mn1–N18	2.3557(11)
Cl1–Mn1–N11	94.22(3)	Cl1–Mn1–N18	165.69(3)	Cl1–Mn1–Cl1a	95.423(18)
Cl1–Mn1–N11a	98.47(3)	Cl1–Mn1–N18a	91.42(3)	N11–Mn1–N18	72.31(4)
N11–Mn1–N11a	161.11(4)	N11–Mn1–N18a	93.53(4)	N18–Mn1–N18a	84.79(4)
For **2** (a: $2 - x, -y, -z$)					
Mn1–Cl1	2.5684(6)	Mn1–Cl2	2.4451(6)	Mn1–N1	2.3680(18)
Mn1–N11	2.3008(17)	Mn1–N21	2.2676(17)	Mn1–Cl1a	2.5950(6)
Cl1–Mn1–Cl2	97.06(2)	Cl1–Mn1–N1	100.28(5)	Cl1–Mn1–N11	167.14(5)
Cl1–Mn1–N21	92.04(5)	Cl1–Mn1–Cl1a	83.576(19)	Cl2–Mn1–N1	157.39(5)
Cl2–Mn1–N11	93.33(5)	Cl2–Mn1–N21	91.53(5)	Cl1a–Mn1–Cl2	103.32(2)
N1–Mn1–N11	71.81(6)	N1–Mn1–N21	73.54(6)	Cl1a–Mn1–N1	92.97(4)
N11–Mn1–N21	95.24(6)	Cl1a–Mn1–N11	86.69(4)	Cl1a–Mn1–N21	164.90(5)
Mn1–Cl1–Mn1a	96.426(19)				
For **3**					
Br1–Mn1	2.6224(7)	Mn1–Br2	2.5048(7)	Mn1–O4	2.412(3)
Mn1–N1	2.332(3)	Mn1–N11	2.257(3)	Mn1–N21	2.241(3)
Br1–Mn1–Br2	102.56(2)	Br1–Mn1–O4	165.71(8)	Br1–Mn1–N1	93.09(9)
Br1–Mn1–N11	89.76(9)	Br1–Mn1–N21	97.33(8)	Br2–Mn1–O4	91.38(8)
Br2–Mn1–N1	164.35(9)	Br2–Mn1–N11	106.26(8)	Br2–Mn1–N21	104.67(8)
O4–Mn1–N1	72.98(12)	O4–Mn1–N11	83.27(11)	O4–Mn1–N21	81.90(11)
N1–Mn1–N11	73.09(11)	N1–Mn1–N21	73.21(11)	N11–Mn1–N21	145.86(11)
For **4**					
Mn1–Br1	2.5637(4)	Mn1–Br2	2.7132(4)	Mn1–O1	2.1890(19)
Mn1–O4	2.2401(18)	Mn1–N1	2.381(2)	Mn1–N11	2.281(2)
Br1–Mn1–Br2	97.678(14)	Br1–Mn1–O1	100.32(6)	Br1–Mn1–O4	91.62(5)
Br1–Mn1–N1	158.27(5)	Br1–Mn1–N11	92.76(5)	Br2–Mn1–O1	88.10(6)
Br2–Mn1–O4	88.02(5)	Br2–Mn1–N1	98.30(5)	Br2–Mn1–N11	167.99(6)
O1–Mn1–O4	167.83(7)	O1–Mn1–N1	94.83(8)	O1–Mn1–N11	84.18(7)
O4–Mn1–N1	74.34(7)	O4–Mn1–N11	97.65(7)	N1–Mn1–N11	73.28(7)
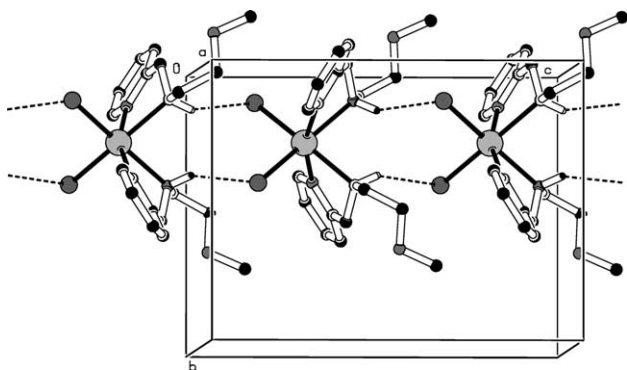
Fig. 2. PLUTON view of the hydrogen bonding in **1**. The monomeric [MnCl$_2$(mepma)$_2$] molecules are linked by N–H$\cdots$Cl hydrogen bonds to form one-dimensional chains that run along the *c*-direction.

ligand N–Mn–N bite angle of 72.31(4)° is also similar to that of 73.26(6)° in [Mn(μ-Cl)$_2$(mppma)]$_n$ [19]. The distance between Mn(II) and the terminal chloride ion in **1** is 2.4810(4) Å, shorter than the distances between Mn(II) and the bridging chlorides in [Mn(μ-Cl)$_2$(mppma)]$_n$ [ranging from 2.5265(6) to 2.5906(6) Å] [19].

3.2.2. [MnCl(μ-Cl)(mpbpa)]$_2$ (**2**)

The molecular structure of **2** is depicted in Fig. 3. Selected interatomic distances and bond angles are listed in Table 2. The molecular structure consists of two centrosymmetrically related Mn(II) centres bridged almost symmetrically by two chloride ions [Mn–Cl(1) = 2.5684(6), Mn–Cl(1a) (a: $2 - x, -y, -z$) = 2.5950(6) Å]. The mpbpa molecule behaves as a tridentate ligand, with the oxygen of the methoxypropyl arm uncoordinated. The three nitrogen atoms of mpbpa adopt the *fac* conformation around the Mn(II) ion. Each Mn(II) ion is additionally coordinated by a terminal chloride, giving a six-coordinate N$_3$Cl$_3$ donor set. As in **1**, the Mn–N distances for the two pyridine nitrogen atoms, N(11) [2.3008(17) Å] and N(21) [2.2676(17) Å], are considerably

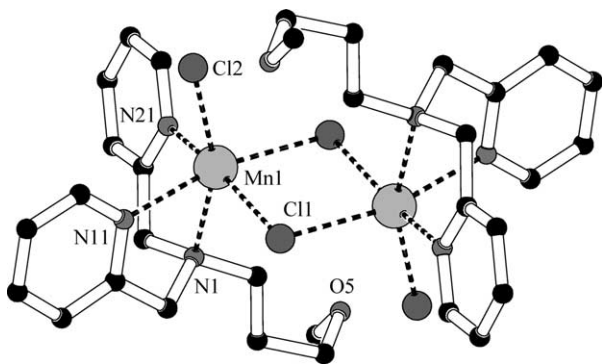shorter than for the tertiary amine N(1) [2.3680(18) Å]. The bridging Mn–Cl bonds are, as expected, slightly elongated, while the terminal Mn–Cl bond [2.4451(6) Å] is normal for octahedral Mn(II) complexes [26]. The Mn$\cdots$Mn distance in **2** [3.8500(6) Å] is comparable to those found in other doubly chloride-bridged dimanganese(II) complexes [27,28].

3.2.3. [MnBr$_2$(mebpa)] (**3**)

In complex **3**, the coordination mode of the mebpa ligand differs significantly from that of the similar mpbpa ligand in **2**; here, the mebpa ligand is tetradentate, with the methoxyethyl oxygen acting as a donor atom. The carbon atoms in the methoxyethyl chain of mebpa are disordered over two sets of positions. The molecular structure of **3**, showing only the major disorder component of the methoxyethyl chain, is presented in Fig. 4. Selected bond lengths and angles are given in Table 2. The three nitrogen atoms of mebpa adopt the *mer* conformation around Mn(II). As above, distances to the Mn(II) ion are shorter for the pyridyl nitrogens, N(11) [2.257(3) Å] and N(21) [2.241(3) Å], than for the tertiary amine nitrogen, N(1) [2.332(3) Å]. The bond distance between the manganese ion and the ether oxygen atom, 2.412(3) Å, is quite long when compared to other such distances [29]. The Mn–Br distance involving the bromide anion opposite to the ether oxygen [Mn–Br(1) = 2.6224(7) Å] is significantly longer than that involving the bromide anion opposite to the amine nitrogen atom [Mn–Br(2) = 2.5048(7) Å].

3.2.4. [MnBr$_2$(MeOH)(Hmepap)] (**4**)

The molecular structure of complex **4** is shown in Fig. 5. Selected geometric data are presented in Table 2. The Mn(II) centre is six coordinate, with one coordination site occupied by the oxygen atom of a methanol molecule. The tridentate coordination of Hmepap is highly unusual: unexpectedly, the ether oxygen of the methoxyethyl arm, rather than the phenol oxygen atom,

Fig. 3. PLATON projection of **2**, with relevant labelling. Hydrogen atoms have been omitted for clarity.
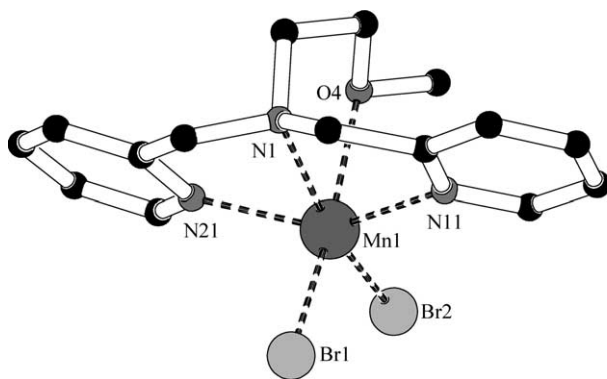

Fig. 4. PLATON projection of **3**, with relevant atomic labelling. Only the major disorder component of the methoxyethyl chain is shown. Hydrogen atoms have been omitted for clarity.
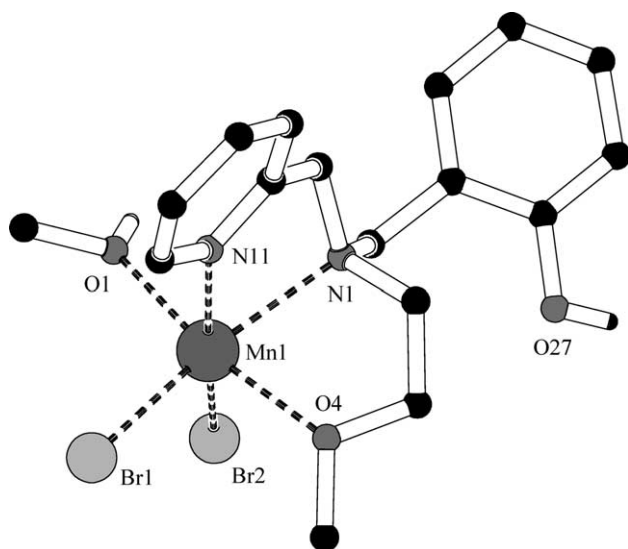
Fig. 5. PLATON projection of **4**, with relevant atomic labelling. Hydrogen atoms, except the one attached to the phenol oxygen, have been omitted for clarity.

binds to the metal ion. The three donating atoms of Hmepap are arranged in the *fac* conformation around manganese. Here, again, the pyridine Mn–N(11) distance [2.281(2) Å] is shorter than the tertiary amine Mn–N(1) distance [2.381(2) Å]. The Mn–O(4) distance involving the ether oxygen atom [2.2401(18) Å] is remarkably shorter than the corresponding distance in **3**, most likely due to the lesser steric hindrance in **4**. The methanol Mn–O(1) bond length [2.1890(19) Å] is shorter than Mn–O(4). The two Mn–Br bond lengths are quite different: the Mn–Br(2) bond [2.7132(4) Å] opposite to the pyridine N(11) is longer than the Mn–Br(1) bond [2.5637(4) Å] opposite to the amine N(1). This may be explained by the *trans* effect of the pyridine N(11), which is more strongly donating than the amine nitrogen N(1). Furthermore, the Br(2) ion participates in two intermolecular O–H···Br hydrogen bonds, with the methanol oxygen of a neighbouring molecule [Br(2)···O(1a) (a: $2 - x, -y, -z$) = 3.198(2) Å] and with the phenol oxygen of another neighbouring molecule [Br(2)···O(27b) (b: $2 - x, 1 - y, -z$) = 3.337(2) Å]. Via these hydrogen bonds the monomeric complex molecules are linked into chains that run along the *b*-direction, as shown in Fig. 6. The special intermolecular H-bonding pattern is likely to be responsible for the unique coordination mode of this ligand in the present complex.

3.3. EPR spectra

All of the complexes **1**, **2**, **3** and **4** are EPR active. As shown in Fig. 7, a frozen methanol solution of complex **1** exhibits a well-resolved six-line signal ($A \sim 90$ G) centred near $g = 2$, consistent with the hyperfine splitting due to the coupling of the electron spin with $I = 5/2$ of the ^{55}Mn(II) nucleus [30–33]. The low intensity lines
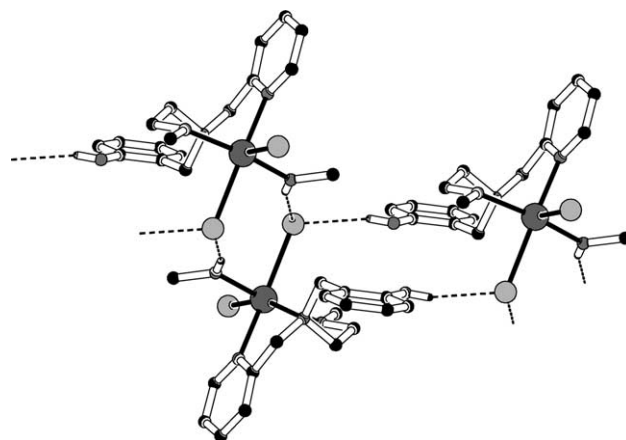

Fig. 6. PLUTON view of the hydrogen bonding in **4**. The monomeric [MnBr$_2$(HOCH$_3$)(Hmepap)] molecules are linked by O–H···Br hydrogen bonds to form one-dimensional chains that run along the *b*-direction.
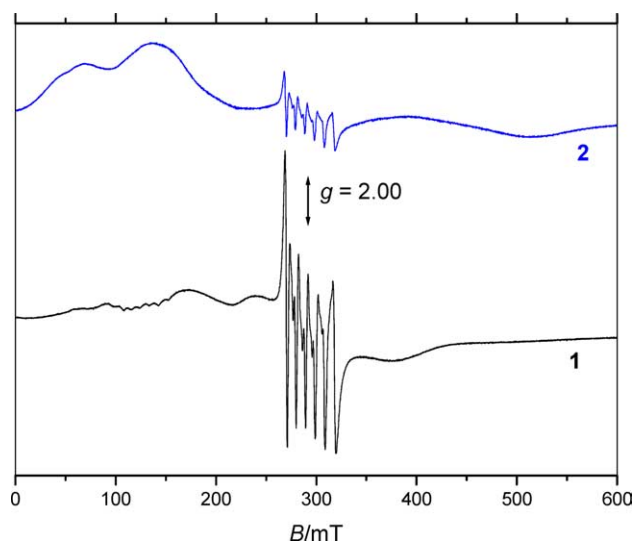

Fig. 7. X-band EPR spectra of frozen solutions of **1** and **2** in methanol.

between the main lines are forbidden transitions due to simultaneous changes of ±1 by both the electronic and the nuclear spin [30,31]. The broad signals above and below $g = 2$ are due to the $S = 5/2$ zero-field splitting, as has been reported for distorted mononuclear Mn(II) complexes [34]. The EPR spectra of frozen methanol solutions of mononuclear **3** and **4** are similar to that of complex **1**. It is noteworthy that for complex **2**, which is a dimer in the solid state, the frozen solution EPR spectrum (Fig. 7) is similar to that of **1**, but in this case the additional bands over a broader range are relatively more intense. These broader bands are very similar to those reported for the analogous dichloro-bridged Mn(II) dimer, [MnCl(μ-Cl)(bpea)]$_2$ [bpea = N,N-bis(2-pyridylmethyl)ethylamine], which exists as a dinuclear entity in dichloromethane solution as well as in the solid state [27], and may thus be ascribed to the presence of dimanganese(II) species [35]. However, the presence of

dinuclear species is hard to prove, as the same broad EPR features may arise from zero-field splitting of a mononuclear species. The EPR spectra of methanol solutions of **2** indicate that decomposition of the dimer to the mononuclear species by the coordinating solvent occurs, although the dimer itself may also be present. The poor solubility of **2** in dichloromethane prevented an EPR measurement of **2** in this solvent.

3.4. Magnetic properties

The temperature dependence of the magnetic susceptibility for the four complexes was studied from 2 to 300 K. Compounds **3** and **4** displayed nearly ideal Curie behaviour. Their χ_M^{-1} versus T plots (χ_M represents molar magnetic susceptibility) are essentially straight lines through the origin. This implies that down to 2 K no magnetic interactions between the Mn(II) ions are present, despite the fact that there are some weak intermolecular hydrogen bonding interactions in **4** (vide supra). The molar effective magnetic moments (μ_{eff}) of **3** and **4** at 300 K are 5.95 and 5.71 μ_B respectively, consistent with an uncoupled high-spin Mn(II) ion whose spin-only value is expected to be 5.92 μ_B.

The magnetic properties of compounds **1** and **2** are more interesting. Plots of the experimental data for both compounds in the forms of χ_M or μ_{eff} per Mn(II) ion versus T are shown in Fig. 8. For **1**, the μ_{eff} value at 300 K is 5.83 μ_B, close to the theoretical value of 5.92 μ_B for an uncoupled high-spin Mn(II) ion. As the temperature is lowered, the μ_{eff} value remains relatively constant to ca. 50 K, then decreases sharply to 1.76 μ_B at 2 K, consistent with the onset of weak antiferromagnetic spin-exchange interactions between the Mn(II) ions through the double hydrogen bonds within the one-dimensional chains. The magnetic susceptibility data may be analysed according to the Fisher's formula for an infinite linear chain of magnetically coupled classical spins scaled to a spin value of 5/2 [5,6,19,36,37]

$$\chi = \frac{Ng^2\beta^2 S(S+1)}{3kT} \frac{1+u}{1-u},$$

$$u = \coth\left[\frac{JS(S+1)}{kT}\right] - \left[\frac{JS(S+1)}{kT}\right]^{-1},$$

where N and β have their usual meanings. A good fit to the experimental data was obtained, giving parameters $J = -1.06$ cm^{-1} and $g = 2.07$, with an agreement factor of $R = 4 \times 10^{-6}$ (R is defined as $\sum[(\chi_M)_{obs} - (\chi_M)_{calc}]^2 / \sum[(\chi_M)_{obs}]^2$) and a coefficient of determination of $r^2 = 0.9992$. The μ_{eff} value of the dinuclear complex **2** is 8.58 μ_B per dinuclear molecule or 6.07 μ_B per Mn(II) at 300 K, values close to the spin-only value for two independent high-spin Mn(II) ions (8.75 μ_B) or one uncoupled high-spin Mn(II) ion (5.92 μ_B). As seen in Fig. 8, the μ_{eff} of **2** increases with decreasing temperature, suggest-
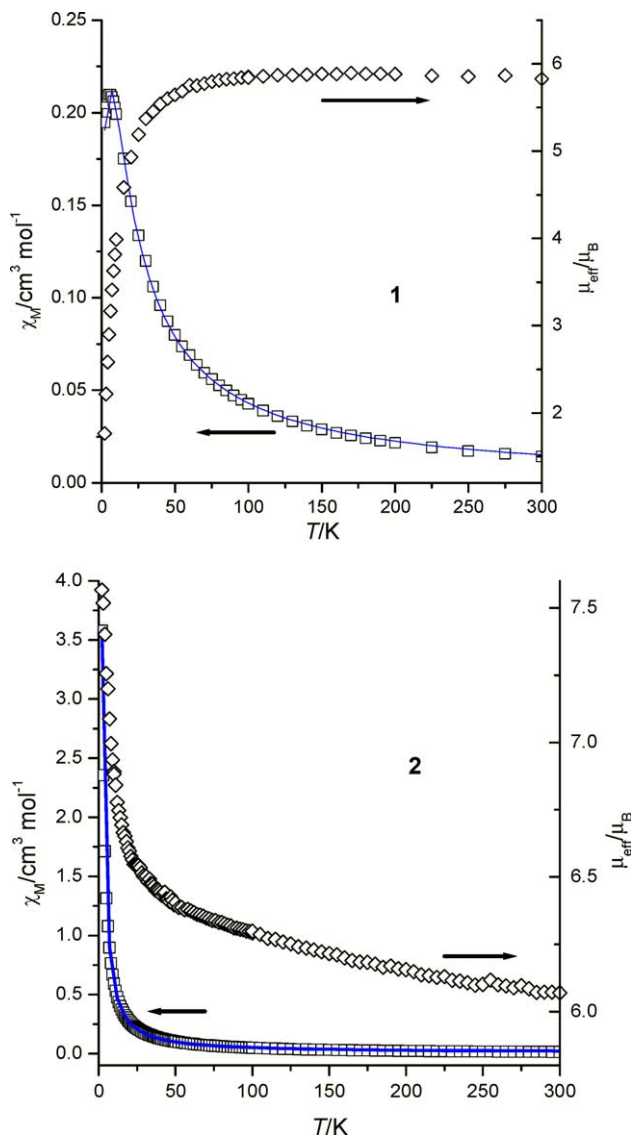

Fig. 8. Temperature dependence of χ_M ($\square$) and μ_{eff} ($\diamond$) per Mn(II) for **1** and **2**. Solid lines are the best fit for χ_M, with $J = -1.06$ cm^{-1}, $g = 2.07$ for **1** and with $J = 0.55$ cm^{-1}, $g = 1.96$ for **2** as described in the text.

ing a ferromagnetic interaction between the pair of Mn(II) ions. The equation for the magnetic susceptibility per Mn(II) for the dinuclear Mn(II) system based on the isotropic Heisenberg model $\boldsymbol{H} = -2J\boldsymbol{S}_1 \cdot \boldsymbol{S}_2$ ($S_1 = S_2 = 5/2$) is given as follows [5,29]

$$\chi_M = \frac{Ng^2\beta^2}{kT} \frac{x^{28} + 5x^{24} + 14x^{18} + 30x^{10} + 55}{x^{30} + 3x^{28} + 5x^{24} + 7x^{18} + 9x^{10} + 11} + N\alpha,$$

where $x = \exp(-J/kT)$, and the other symbols have their usual meanings. The magnetic parameters $g = 1.96$, $J = 0.55$ cm^{-1} and $N\alpha = 0.008$ cm^3/mol are obtained from a fit of the experimental data, with $R = 3 \times 10^{-5}$ and $r^2 = 0.9998$. The small ferromagnetic exchange interaction between the pair of Mn(II) ions is similar in strength to that found for the analogous compound [MnCl(μ-Cl)(bpea)]$_2$ ($J = 0.34$ cm^{-1}) [27].

4. Conclusions

In this study, four new ligands derived from 2-aminomethylpyridine and bearing a methoxyethyl or a methoxypropyl arm, and their complexes with manganese(II) chloride or bromide have been synthesized. Single-crystal X-ray studies have revealed a variety of coordination modes for the ligands. The Mn(II) centre in all four complexes is coordinated in a distorted octahedral fashion. The chloride and bromide ions always serve as coordinating ligands. The oxygen atom in the methoxyethyl or methoxypropyl arm is not necessarily a donor atom. By varying the arm and attaching other potential coordinating moieties such as picolyl or 2-methylphenol groups, these ligands may act as di-, tri- or tetradentate ligands surrounding one Mn(II) centre. The complexes are mono- or dinuclear. The ferro- or antiferromagnetic interactions between the Mn(II) ions through the chloride bridges or hydrogen bonds are very weak.

5. Supplementary material

Crystallographic data (excluding structure factors) have been deposited with the Cambridge Crystallographic Data Centre as supplementary publication no. CCDC-212571 (1), 212572 (2), 212573 (3), and 212574 (4). Copies of the data can be obtained free of charge on application to The Director, CCDC, 12 Union Road, Cambridge, CB2 1EZ, UK (fax: ++/44-1223-336-033; e-mail: deposit@ccdc.cam.ac.uk or http//www.ccdc.cam.ac.uk).

References

[1] V.L. Pecoraro, Manganese redox enzymes, VCH, New York, 1992, p. 141.
[2] N.A. Law, M.T. Caudle, V.L. Pecoraro, Adv. Inorg. Chem. 46 (1999) 305.
[3] J. Wikaira, S.M. Gorun, in: J. Reedijk, E. Bouwman (Eds.), Bioinorganic Catalysis, second ed., Marcel Dekker, New York, 1999, p. 355.
[4] T.G. Carrell, A.M. Tyryshkin, G.C. Dismukes, J. Biol. Inorg. Chem. 7 (2002) 2.
[5] O. Kahn, Molecular Magnetism, Wiley-VCH, 1993.
[6] J.D. Martin, R.F. Hess, Chem. Commun. (1996) 2419.
[7] H. Nagao, M. Nishino, Y. Shigeta, T. Soda, Y. Kitagawa, T. Onishi, Y. Yoshioka, K. Yamaguchi, Coord. Chem. Rev. 198 (2000) 265.
[8] T. Katsuki, Coord. Chem. Rev. 140 (1995) 189.
[9] P. Pietikainen, Tetrahedron 54 (1998) 4319.
[10] J. Brinksma, C. Zondervan, R. Hage, B.L. Feringa, J. Inorg. Biochem. 74 (1999) 82.
[11] R. Hage, J.E. Iburg, J. Kerschner, J.H. Koek, E.L.M. Lempers, R.J. Martens, U.S. Racheria, S.W. Russell, T. Swarthoff, M.R.P. van Vliet, J.B. Warnaar, L. van der Wolf, B. Krijnen, Nature 369 (1994) 637.
[12] S.T. Warzeska, M. Zonneveld, R. van Gorkum, W.J. Muizebelt, E. Bouwman, J. Reedijk, Prog. Org. Coat. 44 (2002) 243.
[13] J.-Z. Wu, E. Bouwman, J. Reedijk, Prog. Org. Coat. 49 (2004) 103.
[14] D.J. Hodgson, K. Michelsen, E. Pedersen, Acta Chem. Scand. 44 (1990) 1002.
[15] G. Roelfes, M. Lubben, S.W. Leppard, E.P. Schudde, R.M. Hermant, R. Hage, E.C. Wilkinson, L. Que Jr., B.L. Feringa, J. Mol. Catal. A 117 (1997) 223.
[16] R.Y.N. Ho, G. Roelfes, K. Hermant, R. Hage, B.L. Feringa, L. Que Jr., Chem. Commun. (1999) 2161.
[17] I. Bernal, I.M. Jensen, K.B. Jensen, C.J. McKenzie, H. Toftlund, J.P. Tuchagues, J. Chem. Soc., Dalton Trans. (1995) 3667.
[18] P. Mialane, A. Nivorojkine, G. Pratviel, L. Azèma, M. Slany, F. Godde, A. Simaan, A. Banse, T. Kargar-Grisel, G. Bouchoux, J. Sainton, O. Horner, J. Guilhem, L. Tchertanova, B. Meunier, J.-J. Girerd, Inorg. Chem. 38 (1999) 1085.
[19] J.-Z. Wu, S. Tanase, E. Bouwman, J. Reedijk, A.M. Mills, A.L. Spek, Inorg. Chim. Acta 351 (2003) 278.
[20] S. Ito, T. Okuno, H. Itoh, S. Ohba, H. Matsushima, T. Tokii, Y. Nishida, Z. Naturforsch. 52 (1997) 719.
[21] A.L. Spek, J. Appl. Crystallogr. 36 (2003) 7.
[22] P.T. Beurskens, G. Beurskens, R. de Gelder, S. García-Granda, R.O. Gould, R. Israel, J.M.M. Smits, The DIRDIF99 Program System, Technical Report of the Crystallography Laboratory, University of Nijmegen, The Netherlands, 1999.
[23] G.M. Sheldrick, SHELXL 97, University of Göttingen, Germany, 1997.
[24] Y.-L. Tong, Y. Yan, E.S.H. Chan, Q. Yang, T.C.W. Mak, D.K.P. Ng, J. Chem. Soc., Dalton Trans. (1998) 3057.
[25] K. Nakamoto, Infrared and Raman Spectra of Inorganic and Coordination Compounds, Part B, fifth ed., Wiley, 1997, p. 58.
[26] A.G. Orpen, L. Brammer, F.H. Allen, O. Kennard, D.G. Watson, R. Taylor, J. Chem. Soc., Dalton Trans. (1989) S1.
[27] I. Romero, M.-N. Collomb, A. Deronzier, A. Llobet, E. Perret, J. Pécaut, L. Le Pape, J.-M. Latour, Eur. J. Inorg. Chem. (2001) 69.
[28] E.M. Meyer, C. Floriani, Angew. Chem. Int. Ed. Engl. 25 (1986) 356.
[29] H. Sakiyama, A. Sugawara, M. Sakamoto, K. Unoura, K. Inoue, M. Yamasaki, Inorg. Chim. Acta 310 (2000) 163.
[30] B.A. Goodman, J.B. Raynor, Adv. Inorg. Chem. Radiochem. 13 (1970) 135.
[31] H.A. Kuska, M.T. Rogers, in: A.E. Martell (Ed.), Coordination Chemistry, Van Nostrand Reinhold, New York, 1971.
[32] J.R. Pilbrow, Transition Ion Electron Paramagnetic Resonance, Oxford University Press, Oxford, 1990.
[33] F.E. Mabbs, D. Collison, Electron Paramagnetic Resonance of d Transition Metal compounds, Elsevier, Amsterdam, 1992.
[34] S.T. Warzeska, F. Miccichè, M.C. Mimmi, E. Bouwman, H. Kooijman, A.L. Spek, J. Reedijk, J. Chem. Soc., Dalton Trans. (2001) 3507.
[35] S.V. Khangulov, P.J. Pessiki, V.V. Barynin, D.E. Ash, G.C. Dismukes, Biochemistry 34 (1995) 2015.
[36] M.E. Fisher, Am. J. Phys. 32 (1964) 343.
[37] H. Iikura, T. Nagata, Inorg. Chem. 37 (1998) 4702.